www.nature.com/cdd

CDDpress

ARTICLE

Check for updates

Targeting HDAC3 to overcome the resistance to ATRA or arsenic in acute promyelocytic leukemia through ubiquitination and degradation of PML-RARα

Bo Dai[1,2,3,6], Feng Wang[2,6], Ying Wang[1,4,6], Jiayan Zhu[1], Yunxuan Li[2], Tingting Zhang[2], Luyao Zhao[2], Lining Wang[1], Wenhui Gao[1], Junmin Li[1], Honghu Zhu[5], Ke Li[2]✉ and Jiong Hu[1]✉

Acute promyelocytic leukemia (APL) is driven by the oncoprotein PML-RARα, which recruits corepressor complexes, including histone deacetylases (HDACs), to suppress cell differentiation and promote APL initiation. All-trans retinoic acid (ATRA) combined with arsenic trioxide (ATO) or chemotherapy highly improves the prognosis of APL patients. However, refractoriness to ATRA and ATO may occur, which leads to relapsed disease in a group of patients. Here, we report that HDAC3 was highly expressed in the APL subtype of AML, and the protein level of HDAC3 was positively associated with PML-RARα. Mechanistically, we found that HDAC3 deacetylated PML-RARα at lysine 394, which reduced PIAS1-mediated PML-RARα SUMOylation and subsequent RNF4-induced ubiquitylation. HDAC3 inhibition promoted PML-RARα ubiquitylation and degradation and reduced the expression of PML-RARα in both wild-type and ATRA- or ATO-resistant APL cells. Furthermore, genetic or pharmacological inhibition of HDAC3 induced differentiation, apoptosis, and decreased cellular self-renewal of APL cells, including primary leukemia cells from patients with resistant APL. Using both cell line- and patient-derived xenograft models, we demonstrated that treatment with an HDAC3 inhibitor or combination of ATRA/ATO reduced APL progression. In conclusion, our study identifies the role of HDAC3 as a positive regulator of the PML-RARα oncoprotein by deacetylating PML-RARα and suggests that targeting HDAC3 could be a promising strategy to treat relapsed/refractory APL.

Cell Death & Differentiation (2023) 30:1320–1333; https://doi.org/10.1038/s41418-023-01139-8

INTRODUCTION

Acute promyelocytic leukemia (APL) is characterized by the PML-RARα fusion gene, which is generated by t(15;17)(q24;q21) chromosomal translocation [1]. The PML-RARα oncoprotein recruits transcription corepressors, such as the N-CoR/SMRT complex and histone deacetylases (HDACs), to impede the cell differentiation program and arrest cells at the promyelocytic stage [1–4]. The combination of all-trans retinoic acid (ATRA) and arsenic trioxide (As_2O_3) or chemotherapy significantly improves the prognosis of APL patients [5]. Mechanistically, As_2O_3 interacts with the PML-RARα protein at the PML-B2 domain to promote the degradation of PML-RARα via SUMOylation and ubiquitylation, and ATRA interacts with PML-RARα at the RARα-LBD domain to reverse the transcriptional repression caused by PML-RARα and thereby induce APL cell differentiation [6–9]. Although the therapeutic strategy of As_2O_3 combined with ATRA highly improves the prognosis of APL, 10–20% of patients are refractory or relapse after treatment [5, 7, 10, 11]. Additionally, most relapsed or refractory patients appear to be ATRA- and/or As_2O_3-resistant and have a poor prognosis [11].

Histone deacetylases (HDACs) are an important class of epigenetic enzymes that regulate gene expression by modulating acetylation modification [12]. A previous study indicated that HDACs, especially HDAC3, act as important components of the PML-RARα transcriptional complex and promote histone 3 (H3) deacetylation, resulting in inhibition of transcription and cessation of cell differentiation in APL cells [13–15]. Furthermore, the NCOR/SMRT complex recruits and stimulates the deacetylase activity of HDAC3 but not other HDAC subtypes, which suggests that HDAC3 can exert special pro-leukemia effects in APL [13, 16–18]. HDAC3 has been identified to play an active role in APL initiating cells, and a pan-inhibitor of HDACs can tackle APL leukemia-initiating cells to relieve APL [19]. However, pan-HDAC inhibitors reveal high toxicity [20]. Therefore, it is necessary to clarify the role and mechanism of HDAC3 in APL cells and whether targeting HDAC3 is effective for the treatment of APL, especially relapsed/refractory APL.

[1]Shanghai Institute of Hematology, Blood and Marrow Transplantation Center, Collaborative Innovation Center of Hematology, Department of Hematology, Ruijin Hospital, Shanghai Jiao Tong University School of Medicine, 197 Ruijin Er Rd, Shanghai 200025, China. [2]NHC Key Laboratory of Biotechnology of Antibiotics, Institute of Medicinal Biotechnology, Chinese Academy of Medical Sciences and Peking Union Medical College, 1 Tian Tan Xi Li, Beijing 100050, China. [3]Department of Hematology, Huashan Hospital, Fudan University, Shanghai 200040, China. [4]Department of Hematology, Tong Ji Hospital, Tong Ji University School of Medicine, No 389 Xincun Road, Shanghai 200065, China. [5]Department of Hematology, The First Affiliated Hospital, College of Medicine, and Institute of Hematology, Zhejiang University, Zhejiang 310003, China. [6]These authors contributed equally: Bo Dai, Feng Wang, Ying Wang. ✉email: like1986@163.com; hj10709@rjh.com.cn

Received: 1 July 2022 Revised: 10 February 2023 Accepted: 20 February 2023
Published online: 9 March 2023

It is well established that PML-RARα ubiquitination and degradation depend on its SUMOylating mediated by PIAS1 [21]. However, the effect of other posttranslational modifications, such as acetylation/deacetylation, on PML-RARα protein stability remains unclear. Here, we demonstrated that the expression of HDAC3 correlated with the expression of PML-RARα rather than HDAC1 or HDAC2 and that HDAC3 maintains the protein stability of PML-RARα. Inhibition of HDAC3 can relieve APL by inducing APL cell differentiation and apoptosis. We further examined how HDAC3 deacetylated PML-RARα and reduced PIAS1-mediated PML-RARα SUMOylation and subsequent RNF4-mediated ubiquitylation. Additionally, we found that HDAC3 inhibition could degrade drug-resistant PML-RARα mutants and relieve As_2O_3-resistant and/or ATRA-resistant APL in vivo and in vitro. Taken together, our study suggests that HDAC3 is a new target for APL treatment and that targeting HDAC3 is an effective strategy for drug-resistant APL.

MATERIALS AND METHODS

Cell lines

Human leukemia NB4 cells and HEK293T cells were purchased from Shanghai Bioleaf Biotech Co., Ltd. NB4-R1 cells and NB4-R2 cells were kind gifts from Kankan Wang (Shanghai Institute of Hematology). All the cells were recently authenticated by STR profiling and characterized by mycoplasma detection and cell vitality detection. NB4, NB4-R1, and NB4-R2 cells were cultured in RPMI 1640 (C11875500, Gibco, Carlsbad, CA, USA) supplemented with 10% fetal bovine serum (FBS) (10270-106, Gibco, Carlsbad, CA, USA), 2 mM L-glutamine, and antibiotics. HEK293T cells were cultured in Dulbecco's modified Eagle's medium (DMEM) (C11995500, Gibco, Carlsbad, CA, USA) with 10% FBS, 2 mM L-glutamine, and antibiotics. Cells were grown at 37 °C in a humidified atmosphere containing 5% CO_2.

Primary patient samples

Primary APL blasts were freshly obtained from the BM tissue of APL patients and healthy donors. Informed consent was obtained from all participants in accordance with the Declaration of Helsinki. The study was approved by the Institutional Review Board of the Ruijin Hospital, Shanghai Jiao Tong University School of Medicine. The clinical features of the patients are listed in Supplementary Table 1.

Mice

NOD.Cg-*Prkdc*^{scid}*Il2rg*^{tm1Sug}/JicCrl (NOG) mice (6–8 weeks old, male; Charles River, Shanghai, China) were used for the NB4 xenograft model, and FVB mice (6–8 weeks old, male; Charles River, Shanghai, China) were used for the *hMRP8-Pml-Rara* transgenic mouse secondary transplantation murine model. For the NB4 xenograft model, 3×10^6 cells/mouse were injected into NOG mice (6–8 weeks old, male; Charles River, Shanghai, China) via the tail vein. One week after transplantation, the mice were randomly separated into four groups ($n = 8$ per group) and treated with either vehicle, RGFP966 (20 mg/kg/d, i.p.) (M2977, Abmole, Houston, TX, USA), ATRA (5 mg/kg/d, p.o.) (M5927, Abmole, Houston, TX, USA), or the combination for three weeks. For the mouse APL model, mouse APL-like spleen cells from *hMRP8-Pml-Rara* transgenic mice were intravenously injected into nonirradiated FVB mice (2×10^5 cells per mouse) aged between 6 and 8 weeks. One week later, mice were randomly separated into four groups and treated with either vehicle, RGFP966 (20 mg/kg/d, i.p.) (M2977, Abmole, Houston, TX, USA), ATRA (5 mg/kg/d, p.o.) (M5927, Abmole, Houston, TX, USA), or the combination for three weeks ($n = 8$ per group). Mice were sacrificed 4 weeks posttransplantation, and peripheral blood, bone marrow, and spleens were analyzed by flow cytometry. Sample size was predetermined empirically according to previous experience using the same strains and treatments, and no particular method of randomization was used. The mice were earmarked before grouping and then were randomly separated into groups by an independent person. We ensured that the experimental groups were balanced in terms of animal age and weight. Experiments were blinded to the person performing analysis. All animal procedures were conducted in accordance with the institutional guidelines, approved by the Institutional Committee for the Ethics of Animal Care and Treatment in Biomedical Research of Chinese Academy of Medical Sciences and PUMC. The animal study was also conducted in accordance with the Animal Research: Reporting of In Vivo Experiments guidelines and the ARRIVE guidelines.

PDX mouse models

For the patient-derived xenograft (PDX) model, four 6-week-old male NOG mice were transplanted with 3×10^6 cells/mouse human ATRA-resistant or As_2O_3-resistant APL cells after 1 Gy irradiation. Four weeks after transplantation, the first-generation mice were killed, peripheral blood and spleen bone marrow were isolated, and leukemia cells were collected. Leukemia cells were tested for human CD45 expression, and the remaining leukemia cells were transplanted into 8 NOG mice with 3×10^6 cells/mouse as the second generation. After stable passage of the third generation, leukemia cells of the fourth generation were transplanted into 30–50 NOG mice (3×10^6 cells/mouse) for in vivo treatment (8–10 mice per group). After confirmation of human leukemia engraftment in murine peripheral blood (>5% human CD45 + cells), mice were treated with either vehicle, RGFP966 (20 mg/kg/d, i.p.) (M2977, Abmole, Houston, TX, USA), ATRA (5 mg/kg/d, p.o.) (M5927, Abmole, Houston, TX, USA), As_2O_3 (2 mg/kg/d, i.p) (311383, Sigma Aldrich, St. Louis, MO, USA) or the combination for three weeks. Mice were sacrificed posttreatment, and peripheral blood, bone marrow, and spleen were analyzed by flow cytometry.

Stable cell lines

To generate NB4 cells stably expressing HDAC3Cas9, the pLenti-L3US2-RFP-HDAC3 plasmid (#83966, Addgene, Watertown, MA, USA) was purchased from Addgene, and the gRNA target sequence was 5′-GTTCTGCTCGCGTTACACGGGTCAATGCCAGGCGAT-3′. This sequence was then cut by Cas9 followed by nonhomologous end-joining (NHEJ). The pLenti-L3US2-RFP-HDAC3 plasmid was cotransfected with the lentiCas9-Blast plasmid (#52962, Addgene, Watertown, MA, USA), and after 24 h of transfection, stable cells were selected in medium containing 1 μg/mL puromycin for 14 days. After 2–3 passages in the presence of puromycin, the cultured cells were used for experiments without cloning.

Selection of NB4-AsR cell line

To generate As_2O_3-resistant NB4 (NB4-AsR) subline, NB4 cells were cultured in 1640 medium supplemented with 0.1 μM As_2O_3 (311383, Sigma Aldrich, St. Louis, MO, USA), and the concentration was gradually increased to 1.5 μM. After 6 months, these cells were stably maintained in the presence of 1.5 μM As_2O_3 and arsenic resistance was achieved. NB4-AsR cells were used in the subsequent experiments.

Reagents and antibodies

RGFP966 (M2977, Abmole, Houston, TX, USA), FK228 (M2007, Abmole, Houston, TX, USA), bortezomib (M1686, Abmole, Houston, TX, USA) and ATRA (M5927, Abmole, Houston, TX, USA) were purchased from Abmole. As_2O_3 (311383, Sigma Aldrich, St. Louis, MO, USA), MG132 (C2211, Sigma Aldrich, St. Louis, MO, USA), and cycloheximide (CHX) (R750107, Sigma Aldrich, St. Louis, MO, USA) were purchased from Sigma Aldrich. For the in vitro experiments, these agents were dissolved in DMSO or sterile water according to the solubility. For the in vivo experiments, RGFP966 and ATRA were dissolved in sterile water with 2% DMSO, 5% Tween 80 and 30% PEG300. Anti-HDAC1 (#34589 S), anti-HDAC2 (#5113 S), anti-HDAC3 (#3949 S), anti-RARα (#62294 S), anti-ubiquitin (#58395 S), anti-PIAS1 (#3550 S), anti-acetylated-lysine (#9441 S) antibodies and mitochondrial dynamic antibodies sampler kit (#74792) were purchased from Cell Signaling Technology (Beverly, MA, USA). Anti-PML (ab179466), anti-PML (ab96051) and anti-PML + RARA (ab43152) fusion antibodies were from Abcam. Anti-PML (NB100-59787) and anti-HDAC3 (NB100-1669) antibodies were purchased from NOVUS (Centennial, CO, USA). Anti-RNF4 (AP16278b) antibody was purchased from ABGENT (San Diego, CA, USA). Anti-SUMO1 (A-716) antibody was purchased from R&D (Minneapolis, MN, USA). Anti-Myc-tagged (562) and anti-HA-tagged (561) antibodies were purchased from MBL BIOTECH (Beijing, China).

Plasmids

The PML-RARα plasmid was a kind gift from Prof. Hugues de Thé's laboratory (Université Paris Diderot, Hôpital St. Louis). PML-RARα drug-resistant mutants (L218P, R276Q, A216V, △F286) were kind gifts from Meidan Ying (Zhejiang University) [22]. Truncations of PML-RARα, △RARα (amino acids 1–394), △PML (amino acids 395–797), △DBD (amino acids 1-797, △416-500), and △LBD (amino acids 1–797, △520–750) were cloned into the pcDNA3.1-myc-His vector by standard subcloning. The pCMV3-HDAC3-HA plasmid (HG11511-CY) was purchased from Sino Biological Inc (Beijing, China). The PML-RARα mutations, including plasmids K65R, K68R, K133R, K150R, K160R, K183R, K209R, K226R, K337R, K380R and K394R, were cloned into the pcDNA3.1-myc-His vector by standard subcloning.

Coimmunoprecipitation, Immunoblotting, Western blotting and Immunostaining

For coimmunoprecipitation, cells were harvested and lysed in buffer containing 50 mM Tris-HCl pH 7.4, 150 mM NaCl, 1 mM EDTA, 1% Triton X-100, 0.25% sodium deoxycholate, 10% glycerol, and 100 μM PMSF and supplemented with protease inhibitor for 30 min at 4 °C. In addition, to analyze the acetylation level, 1 mM trichostatin A (S1045, Selleck, Houston, TX, USA) and 5 mM nicotinamide (S1899, Selleck, Houston, TX, USA) were added to the cell culture medium 6 h in advance and cells lysis buffer. Similarly, to analyze SUMOylation and ubiquitylation levels, cells were pretreated for 6 h with MG132 (C2211, Sigma Aldrich, St. Louis, MO, USA) at a concentration of 10 μM, and MG132 was also added to the cell lysis

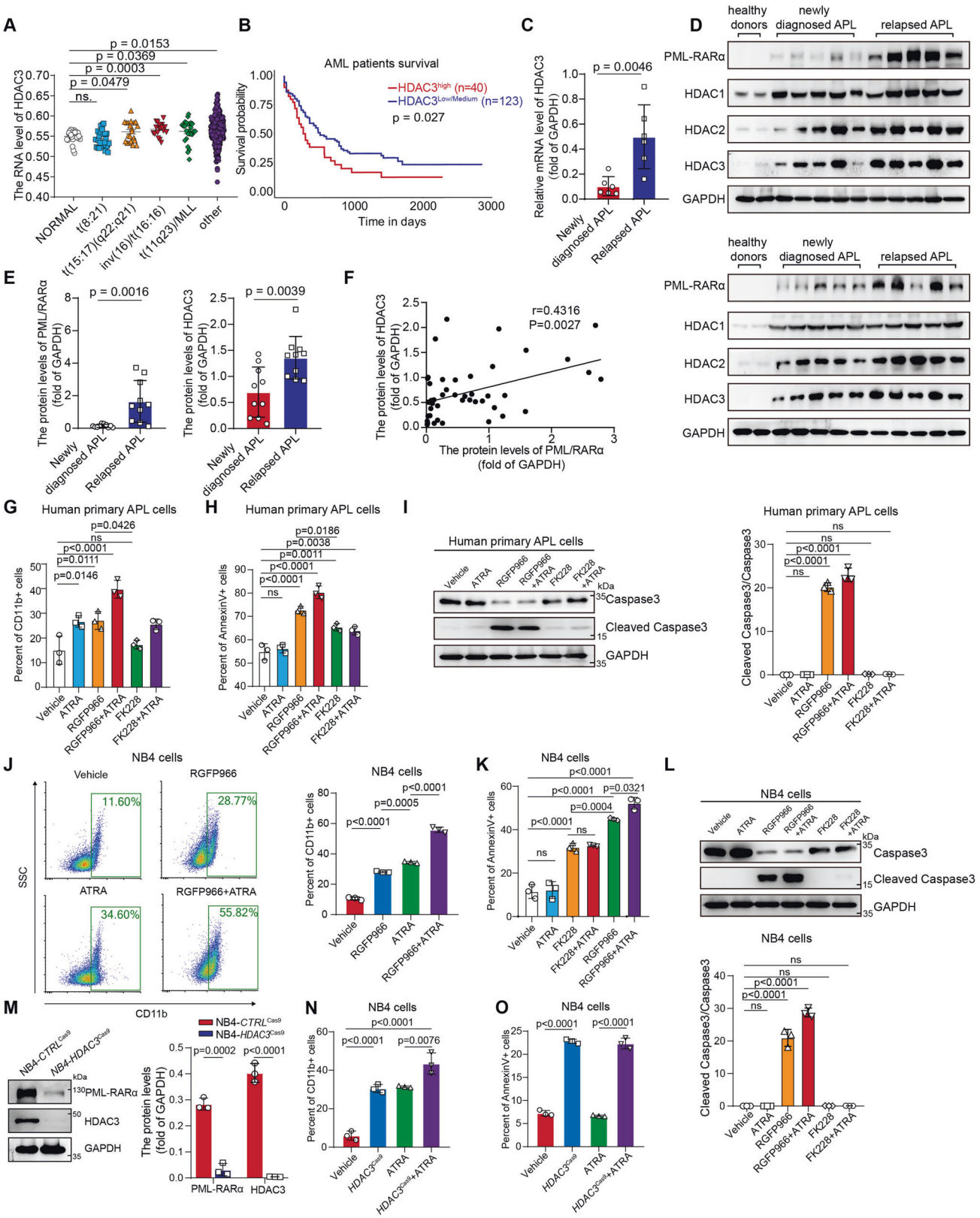

Fig. 1 HDAC3 is highly expressed in the APL subtype, and inhibition of HDAC3 suppresses APL progression by inducing apoptosis and differentiation of APL cells. A The relative mRNA level of *HDAC3* in different chromosomal translocations of AML. Analysis of transcriptomic datasets (GSE13204, mRNA expression normalized to GAPDH). **B** Overall survival of AML patients grouped based on HDAC3 expression; data from the TCGA database were analyzed. **C** The relative mRNA levels of *HDAC3* was detected by quantitative real-time PCR in patients with newly diagnosed and relapsed APL. **D**, **E** Expression of HDACs and PML-RARα was detected by western blotting (WB) in the BM of patients with newly diagnosed and relapsed APL. **F** Correlation between HDAC3 and PML-RARα protein levels in APL patients ($n = 46$). Each data point represents the value from an individual patient. Statistical significance was measured by Pearson's correlation test. **G** Flow cytometry analysis of CD11b expression in human primary APL cells treated with HDAC1 and HDAC2 inhibitors (FK228) or HDAC3 inhibitor (RGFP966) in the presence of 1 μM ATRA or vehicle. CD11b-positive cells were calculated with FlowJo software. **H** Flow cytometry analysis of the percentage of apoptotic cells in human primary APL cells treated with HDAC1 and HDAC2 inhibitors (FK228) or HDAC3 inhibitor (RGFP966) in the presence of 1 μM ATRA or vehicle. Annexin V-positive cells were quantified with FlowJo software. **I** Inhibiting HDAC3 (RGFP966) increased cleaved-caspase 3 expression in human primary APL cells, and cell lysates were immunoblotted with anti-caspase 3 and anti-cleaved-caspase 3. **J** The HDAC3 inhibitor RGFP966 increased the percentage of NB4 cells with positive staining for CD11b. CD11b expression in the indicated cells was evaluated by flow cytometry. The percentage of CD11b-positive cells was calculated with FlowJo software. **K** Flow cytometry analysis of the percentage of apoptotic NB4 cells treated with HDAC1 and HDAC2 inhibitors (FK228) or HDAC3 inhibitor (RGFP966) in the presence of 1 μM ATRA or vehicle. Annexin V-positive cells were quantified with FlowJo software. **L** HDAC3 inhibition (RGFP966) increased cleaved-caspase 3 expression in NB4 cells. Cell lysates were immunoblotted with anti-caspase 3 and anti-cleaved-caspase 3. **M** The effectiveness of HDAC3 knockout was determined by western blotting in the NB4-*HDAC3*^{Cas9} cell line. **N** *HDAC3* knockout increased the percentage of NB4 cells positively stained for CD11b. CD11b expression in the indicated cells with or without ATRA treatment for 24 h was evaluated by flow cytometry. The percentage of CD11b-positive cells was calculated with FlowJo software. **O** *HDAC3* knockout increased the percentage of apoptotic NB4 cells. The percentage of apoptotic cells in the indicated cells with or without ATRA treatment for 24 h was evaluated by flow cytometry. Annexin V-positive cells were quantified with FlowJo software.

buffer. Then, protein supernatants were collected by centrifugation at 12,000 rpm for 30 min. The protein lysates were incubated with magnetic bead-labeled antibody overnight at 4 °C with constant rotation. The immunoprecipitates were then washed five times with lysis buffer and used for western blotting. For immunoblotting assays, proteins were extracted from cells using RIPA buffer (9806 S, Cell Signaling Technology Beverly, MA, USA). A BCA Protein Assay Kit (P1511, Applygen, Beijing, China) was used to determine protein concentrations. For western blotting, protein lysates were resolved by SDS–PAGE and subsequently transferred to PVDF membranes. Membranes were sequentially probed with primary and secondary antibodies. Western blot images were captured using a Tanon 5200 chemiluminescent imaging system (Tanon, Shanghai, China). For immunofluorescence staining, cells were fixed in 4% buffered paraformaldehyde for 15 min at room temperature, permeabilized with 0.5% Triton X-100 for 15 min, and blocked with 3% BSA for 30 min at 37 °C. Specific binding of primary antibodies was detected using corresponding secondary antibodies. Images were acquired using a confocal microscope (Olympus Microsystems, Tokyo, Japan).

Quantitative real-time PCR

Total RNA was extracted using TRIzol (15596026, Invitrogen, Carlabad, CA, USA) following the manufacturer's instructions. Reverse transcription of the total cellular RNA was carried out using oligo (dT) primers and M-MLV reverse transcriptase (AE301-02, Transgen Biotech, Beijing, China). Total RNA was analyzed with a SYBR Fast qPCR Kit (KK4601, Kapa Biosystems, Cape Town, South Africa) according to the manufacturer's instructions. Data were collected and analyzed with Analytikjena QTOWER (Jena, Thuringia, Germany). Relative expression levels were determined by normalization to GAPDH levels. The primer sequences are shown in Supplementary Table 2.

Cell proliferation assay

For the CCK-8 assay, NB4 cells, NB4-R1 cells, NB4-R2 cells or NB4-AsR cells were seeded at a density of 10,000 cells/well. Cells were treated with ATRA, As_2O_3 or RGFP966 and cultured for 24 h. Subsequently, 10 μl of CCK-8 solution (CK04, Dojindo, Kumamoto, Japan) was added to each well, and the plates were incubated at 37 °C for 2 h. Finally, the absorbance was measured at 450 nm. All experiments were conducted using six replicates.

Colony formation assay

Approximately 5000 NB4-R1 or NB4-R2 cells/well were seeded in 12-well plates using semisolid medium (MethoCult H4536; Stemcell Technologies, Cambridge, MA, USA) according to the manufacturer's instructions. Colony formation and numbers were calculated 7 days later.

Flow cytometry

For granulocytic differentiation and apoptosis assays, 1×10^5 cells were washed with PBS and incubated with anti-mouse/human CD11b-FITC (101206, Biolegend, San Diego, CA, USA) or anti-mouse/human CD11b-APC (101212, Biolegend, San Diego, CA, USA), anti-mouse Gr-1-APC (108412, Biolegend, San Diego, CA, USA) or Annexin V-APC (640920, Biolegend, San Diego, CA, USA) for 15 min. Treated cells were incubated with 50 μg/mL propidium iodide (PI) (550825, BD Biosciences, Franklin Lakes, NJ, USA) for 15 min. Then, the cells were detected using a FACSCanto II flow cytometer (BD, Franklin Lakes, NJ, USA) and analyzed by FlowJo software (version 9.3.2).

Luciferase assay

To assess the transcriptional activity of retinoic acid response element (RARE), NB4 cells were transfected with the pGL3-RAR luciferase reporter (11508ES03, Yeasen, Shanghai, China), pCMV3-HDAC3-HA and pTK-Renilla plasmids. After 24 h of transfection, the cells were harvested with lysis buffer, and luciferase activity was then measured using the Dual-Luciferase Reporter Assay System (E1910, Promega, Madison, WI, USA) according to the manufacturer's instructions.

Statistics

Data are expressed as the mean ± standard error of the mean (SEM). Comparisons between two groups were performed using the unpaired Student's *t* test or one-way ANOVA. The correlation between groups was determined by Pearson's correlation test. The survival rates were analyzed by the Kaplan–Meier method. The sample number (*n*) indicates the number of independent biological samples in each experiment. Sample numbers and experimental repeats are indicated in the figures and figure legends. Generally, all experiments were carried out with $n \geq 3$ biological replicates. $P < 0.05$ was considered statistically significant. Analyses were performed using GraphPad Prism 8 software.

RESULTS

HDAC3 is highly expressed in the APL as well as other subtypes of AML, and HDAC3 inhibition suppresses APL progression by inducing apoptosis and differentiation of APL cells

To identify the role of HDAC1, HDAC2, and HDAC3 in different leukemia subtypes, we investigated the changes in gene expression from the transcriptional datasets of GSE13204. *HDAC3* expression was higher in the AML subtype than in the healthy donors, and there was no significant difference in *HDAC1* and *HDAC2* expression between patients with AML and healthy donors (Fig. S1A). Additionally, *HDAC3* expression was higher in AML with translocations t(15:17), inv(16)/t(16:16), or t(11q23)/MLL than in healthy donors (Fig. 1A). Independent analysis of AML patients ($n = 163$) based on The Cancer Genome Atlas (TCGA) dataset confirmed a significant positive correlation between high HDAC3

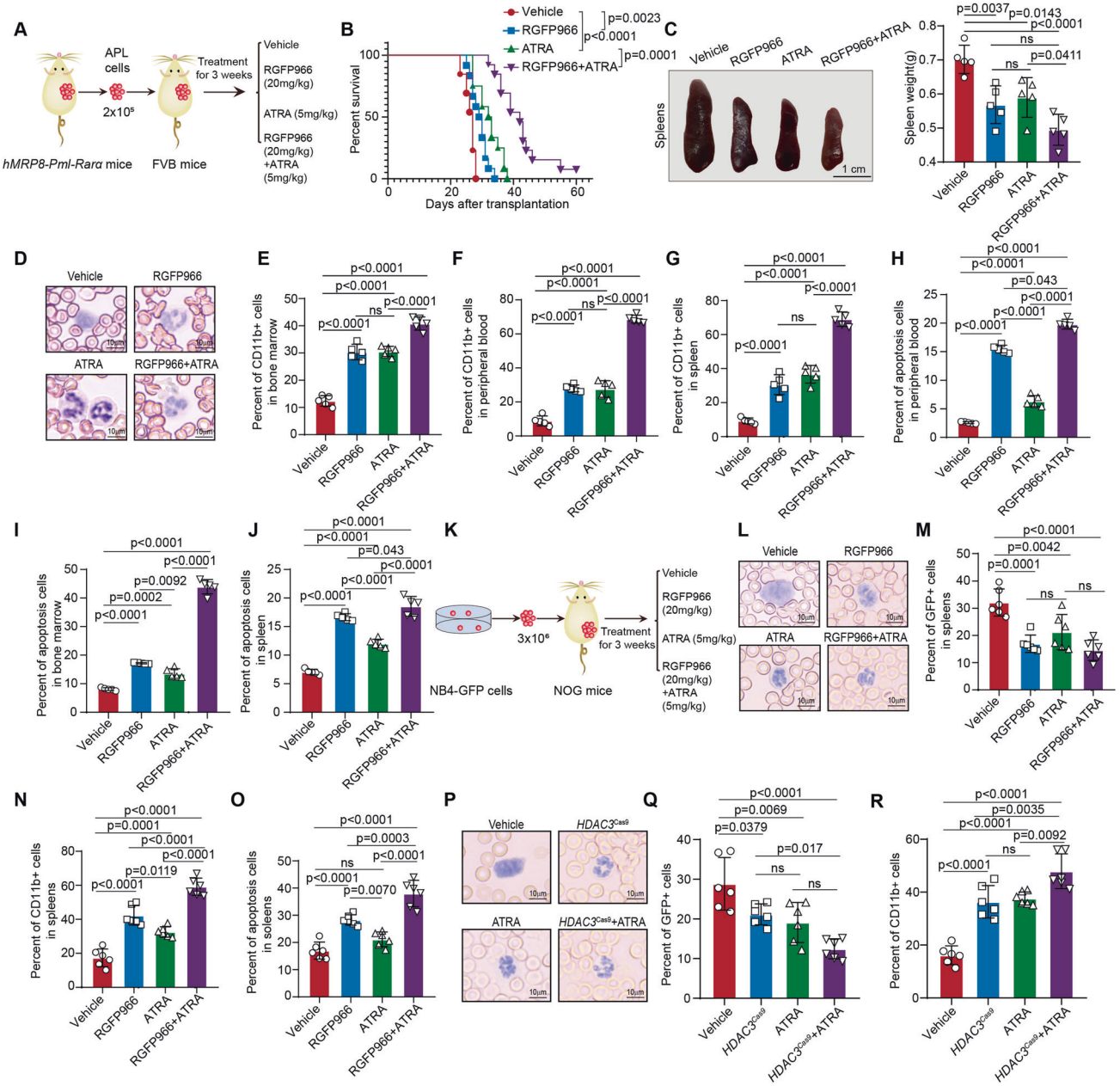

Fig. 2 Inhibition of HDAC3 suppresses APL progression and produces a synergistic effect with ATRA. A The strategy for investigating the anti-APL effects of ATRA, RGFP966, or ATRA combined with RGFP966 treatment on APL cell-transplanted mice in vivo. **B** The survival rate was analyzed by Kaplan–Meier analysis at the end of 60 days. **C** Representative spleens and statistical analyses of spleen weights obtained from mice with the indicated treatment. Scale bar, 1 cm. **D** Representative images of Wright-Giemsa-stained peripheral blood smears of the indicated groups after 21 days of treatment in vivo. (Scale bar, 10 μm). **E**–**G** The indicated treatment induced differentiation of APL cells in the spleen, bone marrow and peripheral blood, as assessed by flow cytometry after 21 days of treatment in vivo. CD11b-positive cells were calculated with FlowJo software. **H**–**J** The indicated treatment induced apoptosis of APL cells in the spleen, bone marrow, and peripheral blood, as assessed by flow cytometry after 21 days of treatment in vivo. Annexin V-positive cells were quantified with FlowJo software. **K** Strategy for evaluation of the anti-APL effects of RGFP966 and/or ATRA treatment in a xenograft transplantation model in vivo. NOG mice were injected intravenously with 3×10^6 GFP-labeled NB4 (NB4-GFP) cells. One week later, the mice were treated with RGFP966 and/or ATRA for 21 days. **L** Representative images of Wright-Giemsa-stained peripheral blood smears of the indicated groups after 21 days of treatment in vivo. (Scale bar, 10 μm). **M** The percentage of leukemia cells in the spleens of NOG mice with the indicated treatment was analyzed by flow cytometry. GFP-positive cells were calculated with FlowJo software. **N** The indicated treatment induced the differentiation of APL cells, as assessed by flow cytometry after 21 days of treatment in vivo. The percentage of GFP- and CD11b-positive cells in spleens was calculated with FlowJo software. **O** Leukemia cells from NOG mice transplanted with NB4 cells treated with RGFP966, ATRA, or ATRA plus RGFP966 were analyzed using flow cytometry for the percentage of apoptotic cells, and the data were analyzed with FlowJo software. **P** Representative images of Wright-Giemsa-stained peripheral blood smears of the indicated groups after 21 days of treatment in vivo. (Scale bar, 10 μm). **Q** Percentage of leukemia cells in the spleens of NOG mice transplanted with NB4-GFP and NB4-*HDAC3*^{Cas9}-GFP cells after 21 days of treatment with or without ATRA. The percentage of GFP-positive cells in spleens was calculated with FlowJo software. **R** The indicated treatment induced the differentiation of APL cells, as assessed by flow cytometry after 21 days of treatment in vivo. The percentage of CD11b-positive cells in spleens was calculated with FlowJo software.

expression (10%) but not HDAC1 or HDAC2 and poor survival of patients with AML (Fig. 1B, Fig. S1B).

In addition, we analyzed the transcription levels of *HDAC1*, *HDAC2*, *HDAC3*, and *PML-RARα* between the initial and relapse stages of the same APL patient ($n = 6$). We observed higher expression of *HDAC2*, and *HDAC3* and lower expression of *HDAC1* in relapsed APL than in the initial APL at the mRNA level (Fig. 1C, Fig. S1C). Consistently, protein levels of PML-RARα, HDAC2, and HDAC3 were elevated in relapsed APL bone marrow samples, and HDAC1 expression did not change in relapsed APL compared with initial APL (Fig. 1D, E, S1D). Moreover, high HDAC3 expression was positively correlated with the expression of PML-RARα in APL patients ($n = 46$, Fig. 1F, Fig. S1E). Taken together, these data indicated that HDAC3 might play an important role in PML-RARα-driven APL.

We further explored the effects of inhibiting HDAC1 and HDAC2 or HDAC3 alone in primary human APL cells or the NB4 cell line. The HDAC1 and HDAC2 inhibitor FK228 or the HDAC3 inhibitor RGFP966 was used to treat these APL cells [23, 24]. In primary human APL cells, inhibition of HDAC1 and HDAC2 with FK228 induced apoptosis but not differentiation, and inhibition of HDAC3 with RGFP966 induced both apoptosis and differentiation (Fig. 1G, H). Moreover, the expression of cleaved caspase 3 was induced by HDAC3 inhibition rather than by HDAC1 or HDAC2 inhibition (Fig. 1I). Additionally, FK228 treatment did not produce a significant change in the ratio of cell differentiation, but RGFP966 treatment exerted significant effects on APL cell differentiation and produced synergistic effects of cell differentiation induction with ATRA in NB4 cells (Fig. 1J, S1F). Similarly, there was a higher percentage of apoptotic NB4 cells treated with FK228

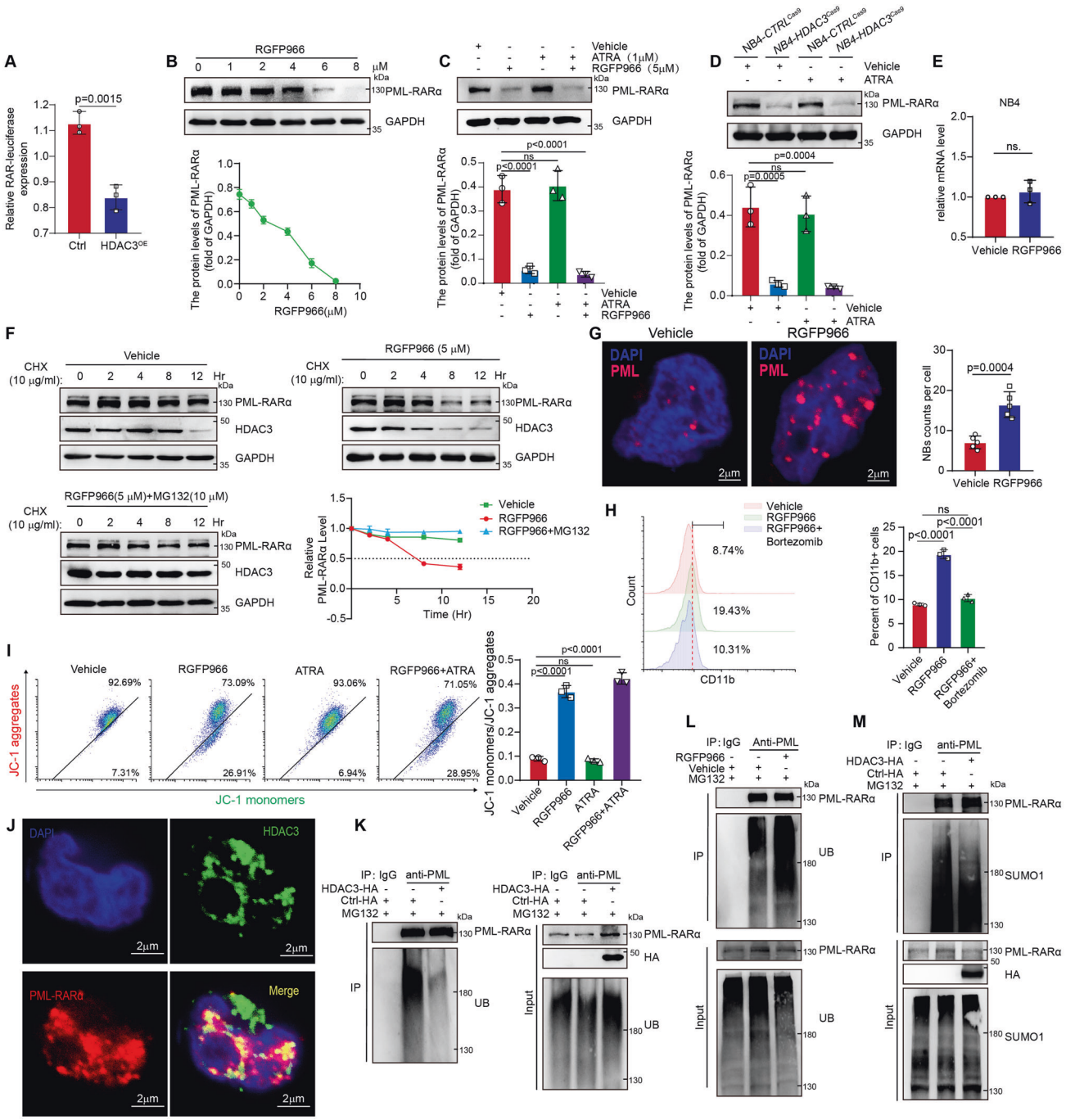

Fig. 3 Inhibition of HDAC3 induces PML-RARα degradation by enhancing ubiquitination. A Effects of HDAC3 overexpression on the transcriptional activity of RARE. Ctrl and HDAC3^{OE} NB4 cells were transfected with the RAR luciferase reporter plasmid, and pTK-Renilla was used as an internal control. After 24 h of transfection, relative luciferase activities (R.L. A) were measured. **B** Inhibiting HDAC3 (RGFP966) reduced PML-RARα expression in a dose-dependent manner. NB4 cells were treated with the indicated concentration of RGFP966, and lysates were immunoblotted with anti-PML-RARα. **C** Synergetic effect of RGFP966 and ATRA on PML-RARα expression. NB4 cells were treated with 5 μM RGFP966 and/or 1 μM ATRA for 24 h. The indicated proteins were detected by immunoblotting. **D** Synergetic effect of HDAC3 knockout and ATRA on PML-RARα expression. NB4 and *HDAC3*^{Cas9} cells were treated with or without ATRA (1 μM) for 24 h. The indicated proteins were detected by immunoblotting. **E** Effect of HDAC3 inhibition on the mRNA level of *PML-RARα*. qRT–PCR was performed to analyze the mRNA levels of *PML-RARα* (normalized to GAPDH) in NB4 cells with or without RGFP966 treatment. **F** Effect of HDAC3 inhibition on PML-RARα degradation in NB4 cells. NB4 cells were treated with or without RGFP966 (5 μM), and 12 h later, the cells were incubated with CHX (10 μg/mL) or CHX plus MG132 (10 μM) for the indicated times. Data are means ± S.E. from three independent experiments. **G** Inhibition of HDAC3 increased the number and size of PML-NBs in NB4 cells. PML-NBs in the indicated NB4 cells were detected by immunofluorescence. Scale bar, 2 μm. **H** Effect of RGFP966 combined with an inhibitor of the proteasome bortezomib on the differentiation of NB4 cells. NB4 cells were treated with RGFP966 (5 μM) or RGFP966 (5 μM) plus bortezomib (10 nM) for 24 h. CD11b expression was evaluated by flow cytometry, and the percentage of CD11b-positive cells was calculated with FlowJo software. **I** Mitochondrial membrane potential change was labeled by JC-1 in NB4 cells with indicated treatment. **J** Colocalization of PML-RARα and HDAC3 in NB4 cells was detected by immunostaining. Scale bar, 2 μm. **K** Effect of HDAC3 on PML-RARα ubiquitylation. NB4 cells were transfected with the indicated plasmids and treated with or without RGFP966 (5 μM), and cell extracts were immunoprecipitated (IP) with rabbit immunoglobulin G (IgG) or anti-PML Ab. Ubiquitinated PML-RARα was detected by immunoblotting. **L** Inhibition of HDAC3 increased PML-RARα ubiquitination. NB4 cells were treated with or without RGFP966 (5 μM), and cell extracts were immunoprecipitated (IP) with rabbit immunoglobulin G (IgG) or anti-PML Ab. Ubiquitinated PML-RARα was detected by immunoblotting. **M** Effect of HDAC3 on PML-RARα SUMOylation. NB4 cells were transfected with the indicated plasmids, and cell extracts were IP with IgG or anti-PML Ab. SUMOylated PML-RARα was detected by immunoblotting.

than in the vehicle group, but after RGFP966 treatment, the percentage of apoptotic cells was much higher than that after FK228 treatment, and only RGFP966 but not FK228 produced synergistic effects with ATRA (Fig. 1K). Meanwhile, the level of cleaved caspase 3 in NB4 cells treated with RGFP966 was significantly higher than those treated with FK228 (Fig. 1L). In addition, *HDAC3* knockout promoted the differentiation and apoptosis of NB4 cells with or without ATRA treatment (Fig. 1M–O). These data indicated that targeting HDAC3 but not HDAC1 or HDAC2 was a more effective therapeutic strategy by inducing APL cell differentiation and apoptosis.

To examine the effects of HDAC3 inhibition on APL cells in vivo, normal FVB mice were transplanted with APL cells from *hMRP8-PML-RARα* mice (Fig. 2A). After treatment for 3 weeks, RGFP966 resulted in the extended survival of mice with APL and combined with ATRA further prolonged the survival time of APL mice compared with the single treatment of ATRA (Fig. 2B). The size of the spleens in the RGFP966 group was smaller than that in the vehicle group mice, and the spleen weight in the RGFP966 combined with ATRA group mice was further reduced much more than that in the ATRA group (Fig. 2C). Wright-Giemsa staining of blood cells and bone marrow showed reduced numbers of immature cells in the RGFP966, ATRA or ATRA plus RGFP966 groups compared with the vehicle group (Fig. 2D, Fig. S2A). Flow cytometry analysis revealed that CD11b-positive (CD11b+) APL cells increased in bone marrow, spleen and peripheral blood in the RGFP966 or ATRA group compared with the vehicle group. Moreover, RGFP966 combined with ATRA resulted in a higher percentage of CD11b + APL cells (Fig. 2E–G). In addition, the percentage of apoptotic cells in bone marrow, spleen and peripheral blood was highest for the RGFP966 plus ATRA group among the APL mice treated with RGFP966 and/or ATRA, indicating that dual treatment with ATRA and RGFP966 enhanced the therapeutic potential of ATRA in APL mice (Fig. 2H–J).

Furthermore, an APL xenograft mouse model was utilized to verify the effect of HDAC3 inhibition. Human APL NB4 cells transduced with GFP lentivirus were intravenously transplanted into NOD.Cg-*Prkdc*^{scid}*Il2rg*^{tm1Sug}/JicCrl(NOG) mice (Fig. 2K). The APL burden and the differentiation and apoptosis of APL cells were detected in the bone marrow of these APL mice. HDAC3 inhibition and/or ATRA induced antileukemic effects, with reduced spleen size, increased cell differentiation, decreased APL cell infiltration, and increased CD11b-positive and apoptotic cells (Fig. 2L–O, Fig. S2B, C). In particular, the combination of an HDAC3 inhibitor with ATRA had synergistic antileukemic effects in this model (Fig. 2L–O, Fig. S2B, C). Similar to the observation with the HDAC3 inhibitor treatment, *HDAC3* deletion in APL cells (Fig. S2D) reduced the spleen involvement with APL compared with the vehicle group (Fig. S2E). Wright-Giemsa staining of APL cells in peripheral blood and bone marrow smears showed that cells with *HDAC3* knockout developed a differentiated morphology (Fig. 2P, Fig. S2F). The percentage of GFP + APL cells was decreased in the *HDAC3* deletion group (Fig. 2Q). Additionally, *HDAC3* knockout induced differentiation and apoptosis in APL cells (Fig. 2R, S2G). ATRA exerted a more remarkable antileukemic effect on *HDAC3*-deleted APL cells than on vehicle APL cells in vivo (Fig. 2Q, R). Collectively, these results revealed that HDAC3 could be a new target for the treatment of APL and that the inhibition of HDAC3 promoted the apoptosis and differentiation of APL cells to relieve APL in vivo.

Inhibition of HDAC3 promotes PML-RARα degradation by inducing PML-RARα acetylation and subsequent ubiquitination

To explore the mechanism by which HDAC3 inhibition relieved APL, we first examined whether HDAC3 affected PML-RARα transcriptional activity. We transfected NB4 cells with a retinoic acid receptor luciferase reporter plasmid (RAR-luc) with or without HDAC3 and found that overexpression of HDAC3 decreased RAR-luc activity (Fig. 3A). Interestingly, RGFP966 reduced PML-RARα protein levels in a dose-dependent manner, while ATRA did not decrease PML-RARα expression (Fig. 3B, C). Moreover, knockout of *HDAC3* in NB4 cells showed a similar phenotype to that of HDAC3 inhibition (Fig. 3D). qPCR analysis revealed no significant difference in the transcription level of *PML-RARα* between the vehicle and RGFP966 groups (Fig. 3E). We next examined whether HDAC3 could regulate PML-RARα protein stability. As shown in Fig. S3A, overexpression of HDAC3 increased the half-life of PML-RARα protein degradation. Additionally, inhibition of HDAC3 accelerated PML-RARα degradation in NB4 cells, which was rescued by the proteasomal inhibitor MG132 (Fig. 3F), suggesting that HDAC3 regulated PML-RARα protein stability via the ubiquitin proteasome system.

A previous study has shown that PML-RARα degradation recovers the formation of PML nuclear bodies (PML-NBs) [25], so we next examined whether HDAC3 could regulate PML-NBs assembly. As shown in Fig. 3G, treatment with RGFP966 increased PML-NBs numbers in NB4 cells. Furthermore, treatment with RGFP966 induced NB4 cell pro-differentiation; however, inhibition of the ubiquitin proteasome system by bortezomib rescued the pro-differentiation effect caused by RGFP966 (Fig. 3H). Low

membrane potential mitochondria were observed in NB4 cells treated with RGFP966 compared to the control cells, which means early apoptosis occurred (Fig. 3I). Moreover, mitochondrial dynamics experiments illustrated that HDAC3 inhibition promoted mitochondrial fission (Fig. S3B) [26, 27]. We also found that PML-RARα colocalized with HDAC3 in APL cells (Fig. 3J). HDAC3 overexpression inhibited ubiquitylation of PML-RARα (Fig. 3K), while inhibition of HDAC3 resulted in enhancement of PML-RARα ubiquitylation in NB4 cells (Fig. 3L). In addition, HDAC3 overexpression also reduced SUMOylation of PML-RARα (Fig. 3M). These data indicated that HDAC3 sustained PML-RARα protein stability by interfering with its ubiquitination.

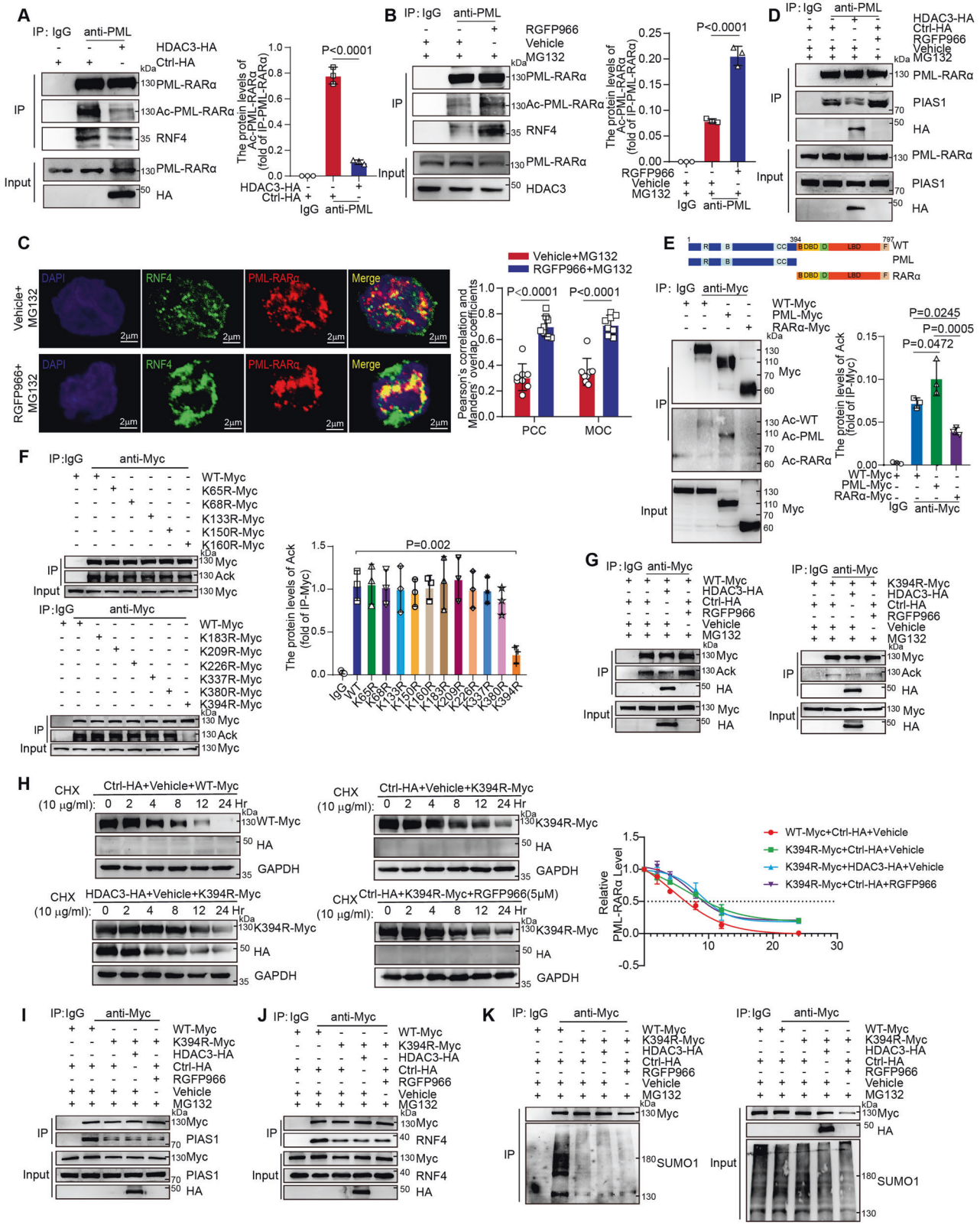

Fig. 4 HDAC3-mediated PML-RARα deacetylation interferes with PML-RARα ubiquitination and degradation. A, **B** Effect of HDAC3 or inhibition of HDAC3 on PML-RARα acetylation and the PML-RARα/RNF4 interaction. NB4 cells were transfected with the indicated plasmid and treated with or without RGFP966, and cell extracts were IP with IgG and anti-PML Ab. **C** Colocalization of PML-RARα and RNF4 was detected by immunostaining in NB4 cells after the indicated treatment for 24 h. Scale bar, 2 μm. **D** Effect of HDAC3 on the PML-RARα/PIAS1 interaction. NB4 cells were transfected with the indicated plasmids and treated with or without RGFP966, and cell extracts were IP with IgG or anti-PML Ab. **E** Mapping the acetylation region of PML-RARα. Top: deletion mutants of PML-RARα (△PML and △RARα domains). Bottom: acetylation of PML-RARα, the PML domain and the RARα domain. HEK293T cells were cotransfected with the indicated PML-RARα constructs. Cell extracts were IP with IgG and anti-Myc Ab. **F** Acetylation sites of PML-RARα. HEK293T cells were transfected with the indicated mutants of PML-RARα. Cell extracts were IP with IgG or anti-Myc Ab. **G** Effect of HDAC3 or the inhibition of HDAC3 on the acetylation of PML-RARα and PML-RARα-K394R. HEK293T cells were cotransfected with the indicated plasmids and treated with or without RGFP966 (5 μM). Cell extracts were IP with IgG or anti-Myc Ab. **H** Effect of HDAC3 or the inhibition of HDAC3 on PML-RARα-K394R degradation. HEK293T cells were transfected with the indicated plasmids and treated with or without RGFP966 (5 μM), and 12 h later, they were incubated with cycloheximide (CHX) (10 μg/mL) for the indicated times. Data are means ± S.E.M from three independent experiments. **I** Effect of HDAC3 or HDAC3 inhibition on the PML-RARα-K394R/PIAS1 interaction. HEK293T cells were transfected with the indicated plasmids and treated with or without RGFP966 (5 μM). Cell extracts were IP with IgG or anti-Myc Ab. **J** Effect of HDAC3 or HDAC3 inhibition on the PML-RARα-K394R/RNF4 interaction. HEK293T cells were transfected with the indicated plasmids and treated with or without RGFP966 (5 μM). Cell extracts were IP with IgG or anti-Myc Ab. **K** Effect of HDAC3 or HDAC3 inhibition on PML-RARα-K394R SUMOylation. HEK293T cells were transfected with the indicated plasmids and treated with or without RGFP966 (5 μM). Cell extracts were IP with IgG or anti-Myc Ab. SUMOylated PML-RARα-K394R was detected by immunoblotting.

Given that HDAC3 is responsible for the deacetylation of lysine residues on core histones and other nonhistone substrates [28], we speculate that HDAC3 interfered with PML-RARα ubiquitylation by affecting the acetylation of PML-RARα. Overexpression of HDAC3 decreased the acetylation of PML-RARα, while inhibition of HDAC3 increased the acetylation of PML-RARα in NB4 cells (Fig. 4A, B). The SUMO-dependent E3 ubiquitin ligase RNF4 polyubiquitinated PML-RARα and subsequently degraded it via the proteasome [29]. We found that HDAC3 overexpression decreased RNF4 binding with PML-RARα (Fig. 4A), while inhibition of HDAC3 increased acetylation of PML-RARα and the interaction of RNF4 with PML-RARα in NB4 cells (Fig. 4B). Immunofluorescence data revealed that more RNF4 co-localized with PML-RARα in HDAC3 inhibitor-treated NB4 cells (Fig. 4C). RNF4 has been reported to bind with the SUMOylated PML moiety of PML-RARα, and this modification is mediated by PIAS1 [21]. In addition, overexpression of HDAC3 repressed the interaction of PIAS1 with PML-RARα, while inhibition of HDAC3 increased their interaction (Fig. 4D). Using deletion mutants of the RARα domain of PML-RARα, we found that HDAC3 interacted with both the DBD and LBD motifs of the RARα domain (Fig. S4A, B). To further explore the specific role of HDAC3 in regulating PML-RARα acetylation modification, we utilized deletion mutants of the PML and RARα domains of PML-RARα and found that an acetylation modification occurred in PML domains of PML-RARα (Fig. 4E). Additionally, the regulation of acetylation modification by HDAC3 depended on its interaction with the RARα domain of PML-RARα (Fig. 4G left, S4C–E).

To determine which lysine was essential for acetylation modification of the PML domain of PML-RARα, we used a series of lysine mutants of PML-RARα (K65R/K68R/K133R/K150R/K160R/K183R/K209R/K226R/K337R/K380R/K394R) to determine the deacetylation modification regulated by HDAC3. We found that the acetylation of K394R was significantly reduced, and the acetylation modification was not affected by overexpression or inhibition of HDAC3 (Fig. 4F, G, Fig. S4E, F). We next examined whether HDAC3 regulated PML-RARα-K394R stability. The results demonstrated that the half-life of PML-RARα-K394R was significantly prolonged compared with that of PML-RARα, and neither overexpression nor inhibition of HDAC3 changed the degradation rate of PML-RARα-K394R (Fig. 4H). In addition, the interaction of PML-RARα-K394R with PIAS1 and RNF4 was reduced compared with that of PML-RARα and was not affected by overexpression or inhibition of HDAC3 (Fig. 4I, J). Furthermore, SUMOylation of PML-RARα-K394R was also significantly reduced compared with PML-RARα and was not affected by overexpression or inhibition of HDAC3 (Fig. 4K). Taken together, inhibition of HDAC3 induced acetylation of PML-RARα lysine 394, thereby enhancing its interaction with PIAS1 and RNF4 and ultimately degradation via the ubiquitin proteasome system.

Inhibition of HDAC3 can relieve drug-resistant APL in vivo and in vitro

Our results revealed that the deacetylated site of PML-RARα by HDAC3 was different from the binding sites of PML-RARα by ATO or ATRA. Therefore, we speculated that targeting HDAC3 could induce antileukemic effects on ATO- or ATRA-resistant APL cells. In primary human APL cells, inhibition of HDAC3 increased the percentage of CD11b + and apoptotic cells in ATO- and ATRA-resistant APL cells, as shown by flow cytometry analysis (Fig. 5A, B). Furthermore, treatment with RGFP966 decreased PML-RARα expression in NB4-R1 and NB4-R2 cells in a dose-dependent manner (Fig. 5C). Inhibition of HDAC3 reduced the proliferation and colony-formation units (CFUs) of NB4-R1 and NB4-R2 cells (Fig. 5D, E). Flow cytometry analysis demonstrated that inhibition of HDAC3 increased differentiation and apoptosis in NB4-R1 and NB4-R2 cells (Fig. 5F, G). Moreover, ATO-resistant NB4 cell subline was derived from NB4 cell line by gradually increasing the dose of As_2O_3 from 0.1 to 1.5 μM (Fig. 5H). NB4-AsR cells showed low sensitivity for As_2O_3 treatment, whereas HDAC3 inhibition with RGFP966 decreased the cell growth of NB4-AsR cells (Fig. 5H) and induced NB4-AsR cells differentiation and apoptosis (Fig. 5I, J). ATO-resistant forms of PML-RARα (A216V and L218P) conferred resistance against ATO-induced degradation [30]. We found that RGFP966 also effectively reduced the protein levels of A216V and L218P mutants and the ATRA-resistant mutants of PML-RARα (ΔF286 and R276Q) (Fig. 5K).

We next identified whether HDAC3 inhibition attenuated drug-resistant APL in vivo. APL xenograft mouse models of NB4-R2 and NB4-AsR cells was used to evaluate the effects of the HDAC3 inhibitor (Fig. 6A, I). After 60 days of treatment, RGFP966 increased the survival rate of drug-resistant APL mice (Fig. 6B). Inhibition of HDAC3 reduced the spleen and liver sizes of APL mice (Fig. 6C). Wright-Giemsa staining of blood cells and bone marrow showed that HDAC3 inhibition induced APL cell differentiation (Fig. 6D, E). A decreased percentage of human CD45 + cells was detected after RGFP966 treatment (Fig. 6F). Furthermore, HDAC3 inhibition increased the percentage of CD11b + and apoptotic APL cells (Fig. 6G, H). However, ATRA treatment showed no significant anti-leukemia effects in this model compared with the vehicle group (Fig. 6B–H). Similarly, Wright-Giemsa staining of bone marrow swear illustrated that RGFP966 induced ATO-resistant cells differentiation (Fig. 6J). Flow cytometry analysis demonstrated that HDAC3 inhibition decreased the percentage of human CD45 + cells and increased the percentage of CD11b + and apoptotic APL cells (Fig. 6K–M). Moreover, patient-derived tumor xenograft (PDX) models were established to explore

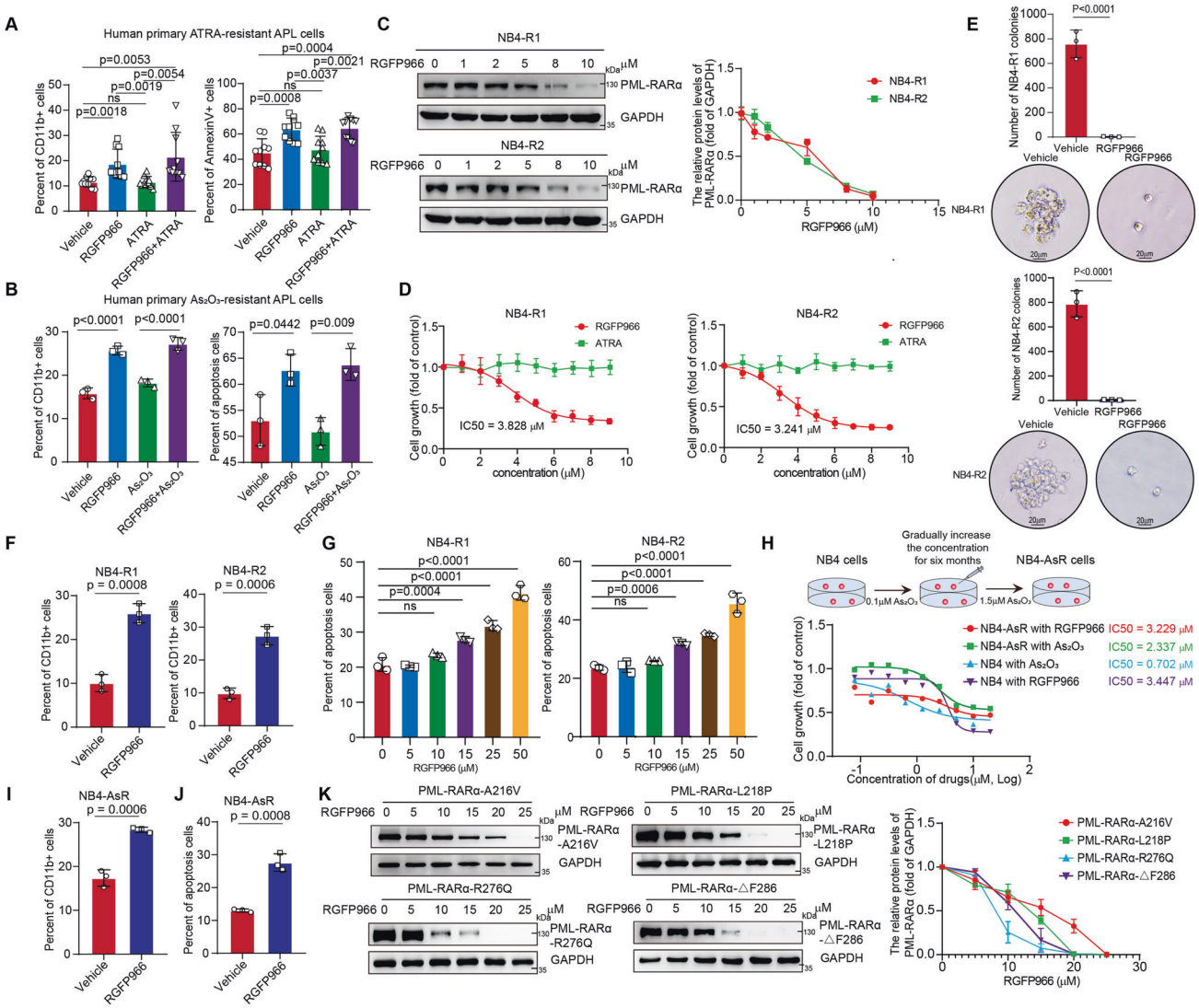

Fig. 5 Inhibition of HDAC3 induces differentiation and apoptosis in drug-resistant APL cells by degrading PML-RARα mutations. A Effect of RGFP966 and/or ATRA on the differentiation and apoptosis of primary ATRA-resistant APL cells. Human primary ATRA-resistant APL cells were treated with RGFP966 and/or ATRA for 24 h and then stained with CD11b or Annexin V/PI. The percentages of CD11b-positive cells and Annexin V-positive cells were calculated with FlowJo software. **B** Effect of RGFP966 and/or ATRA on the differentiation and apoptosis of primary As_2O_3-resistant APL cells. Human primary As_2O_3-resistant APL cells were treated with RGFP966 and/or ATRA for 24 h, and the cells were stained with CD11b or Annexin V/PI. The percentages of CD11b-positive cells and Annexin V-positive cells were calculated with FlowJo software. **C** Inhibiting HDAC3 (RGFP966) reduced PML-RARα expression in a dose-dependent manner. NB4-R1 and NB4-R2 cells were treated with the indicated concentration of RGFP966, and lysates were immunoblotted with anti-PML-RARα. **D** Effects of RGFP966 or ATRA on the viability of NB4-R1 and NB4-R2 cells. Data are a summary of IC50 values for RGFP966. **E** Representative images and colony numbers of NB4-R1 and NB4-R2 cells treated with or without RGFP966 (5 μM). Data are means ± SEM. **F** Effect of RGFP966 on the differentiation of NB4-R1 and NB4-R2 cells. NB4-R1 and NB4-R2 cells were treated with or without RGFP966 (5 μM) for 24 h, and cells were stained with CD11b. The percentage of CD11b-positive cells was calculated with FlowJo software. **G** Effect of RGFP966 on apoptosis of NB4-R1 and NB4-R2 cells. NB4-R1 and NB4-R2 cells were treated with the indicated concentrations of RGFP966, stained with Annexin V/PI and evaluated. The percentage of Annexin-V-positive cells was calculated with FlowJo software. **H** Approaches to generate NB4-AsR cells and effects of RGFP966 or As_2O_3 on the proliferation viability of NB4 and NB4-AsR cells. Data are a summary of IC50 values for RGFP966 and As_2O_3. **I** Effect of RGFP966 on the differentiation of NB4-AsR cells. NB4-AsR cells were treated with or without RGFP966 (5 μM) for 24 h, and cells were stained with CD11b. The percentage of CD11b-positive cells was calculated with FlowJo software. **J** Effect of RGFP966 on apoptosis of NB4-AsR cells. NB4-AsR cells were treated with the indicated concentrations of RGFP966, stained with Annexin V/PI and evaluated. The percentage of Annexin-V-positive cells was calculated with FlowJo software. **K** Effect of RGFP966 on the degradation of PML-RARα drug-resistant mutants (ΔF286, R276Q, L218P and A216V) in vitro. HEK293T cells were transfected with the indicated plasmids for 24 h and treated with the indicated concentrations of RGFP966. After 24 h of treatment, cell lysates were immunoblotted with anti-PML-RARα.

the remission of ATRA- and ATO-resistant APL by targeting HDAC3 (Fig. 6N, Q). In the ATRA-resistant PDX model, the percentage of human CD45 + cells in the spleen were decreased after RGFP966 treatment (Fig. 6O). An increased percentage of CD11b + APL cells in the spleen were detected after RGFP966 treatment (Fig. 6P). Similarly, in the ATO-resistant PDX model, the percentage of human CD45 positive cells decreased, whereas CD11b positive and apoptosis APL cells increased after RGFP966 treatment (Fig. 6R–T and Fig. S5A–C). These data indicated that HDAC3 inhibition showed antileukemia efficacy in ATO- or ATRA-resistant APL.

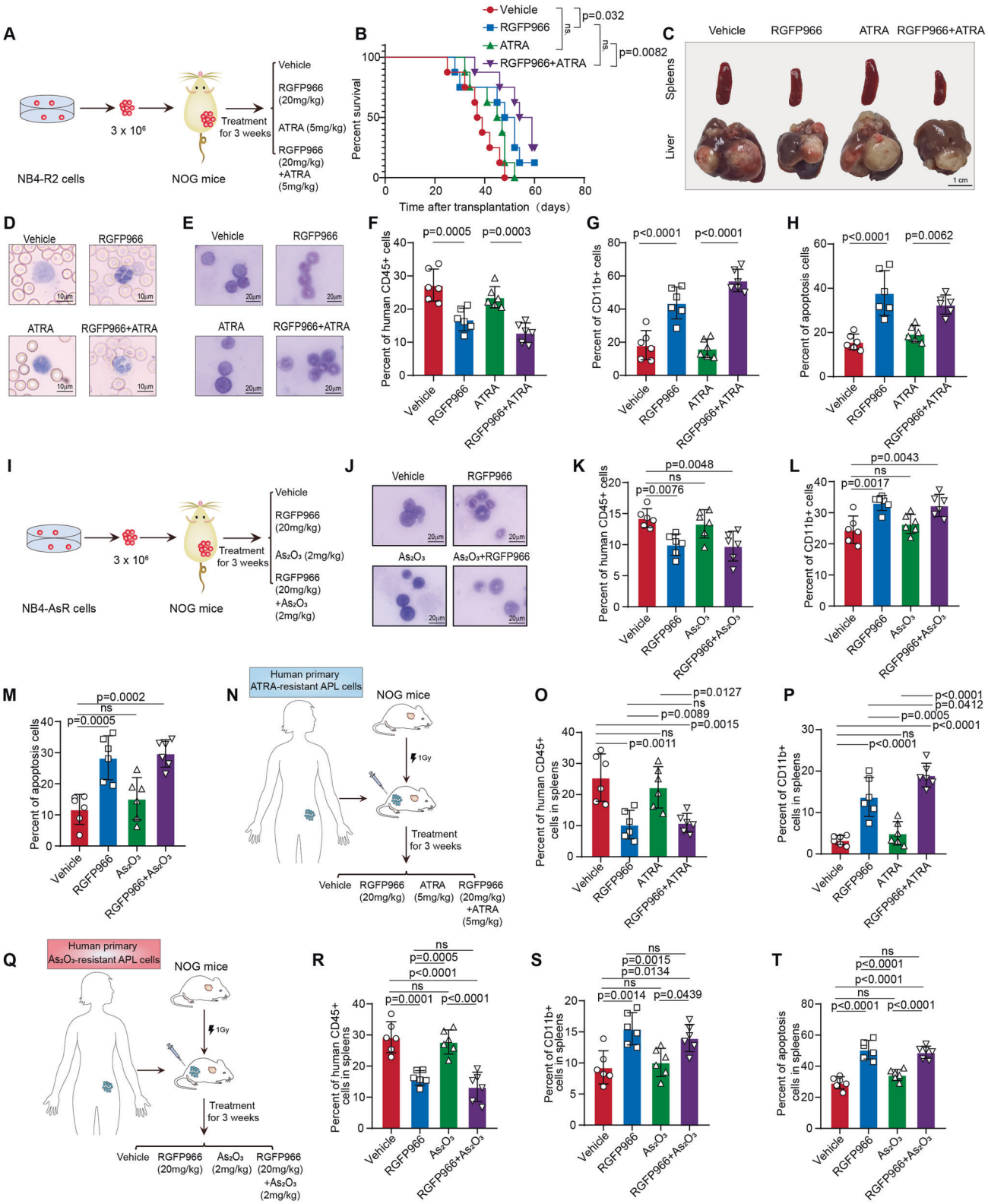

DISCUSSION

The occurrence and development of APL is mainly due to fusion protein PML-RARα-mediated transcriptional repression and PML-NBs formation disruption, causing BM-derived cells to enter an undifferentiated state and undergo malignant proliferation [1]. According to the pathogenesis of APL, the combination of ATRA and AS_2O_3 leads to the degradation of PML-RARα and the formation of PML-NBs, which promotes APL cell differentiation and apoptosis [31]. Thus, over 95% of initial APL can be definitively cured through the combination therapy of ATRA and ATO [1]. However, 10–30% of patients relapse, and many relapsed APL patients are drug resistant [30]. The major purpose of this study

Fig. 6 Inhibition of HDAC3 relieves APL in animal models inoculated with drug-resistant APL cells. A The strategy for investigating the anti-APL effects of ATRA, RGFP966 or ATRA combined with RGFP966 treatment on ATRA-resistant cell-transplanted mice in vivo. **B** The survival rate was analyzed by Kaplan–Meier analysis at the end of 60 days. **C** Representative spleens and livers obtained from NOG mice treated with vehicle, RGFP966, ATRA or ATRA and RGFP966 in the ATRA-resistant xenograft transplantation model. Scale bar, 1 cm. **D**, **E** Representative images of Wright-Giemsa-stained peripheral blood and bone marrow smears of the indicated groups after 21 days of treatment in vivo. (Scale bar, 10 μm). **F** Percentage of leukemia cells in the spleens of NOG mice with the indicated treatment was analyzed by flow cytometry. hCD45-positive cells were calculated with FlowJo software. **G** The indicated treatment induced the differentiation of APL cells, as assessed by flow cytometry after 21 days of treatment in vivo. The percentage of hCD45- and CD11b-positive cells in spleens was calculated with FlowJo software. **H** The indicated treatment induced apoptosis of APL cells, as assessed by flow cytometry after 21 days of treatment in vivo. The percentage of Annexin V-positive cells in spleens was calculated with FlowJo software. **I** The strategy for investigating the anti-APL effects of As_2O_3, RGFP966 or As_2O_3 combined with RGFP966 treatment on As_2O_3-resistant NB4 cell-transplanted mice in vivo. **J** Representative images of Wright-Giemsa-stained bone marrow smears of the indicated groups after 21 days of treatment in vivo. (Scale bar, 20 μm). **K** Percentage of leukemia cells in the spleens of NOG mice with the indicated treatment was analyzed by flow cytometry. hCD45-positive cells were calculated with FlowJo software. **L** The indicated treatment induced the differentiation of APL cells, as assessed by flow cytometry after 21 days of treatment in vivo. The percentage of hCD45- and CD11b- positive cells in spleens was calculated with FlowJo software. **M** The indicated treatment induced apoptosis of APL cells, as assessed by flow cytometry after 21 days of treatment in vivo. The percentage of Annexin V-positive cells in spleens was calculated with FlowJo software. **N** Strategy for constructing patient-derived tumor xenograft (PDX) models from primary ATRA-resistant APL cells. **O** The percentage of human leukemia cells in spleens of ATRA-resistant PDX mice with the indicated treatment was analyzed by flow cytometry. hCD45-positive cells were calculated with FlowJo software. **P** The percentage of CD11b-positive human leukemia cells from ATRA-resistant PDX mice with the indicated treatment was analyzed by flow cytometry. CD11b-positive cells were calculated with FlowJo software. **Q** Strategy for constructing patient-derived tumor xenograft (PDX) models from primary As_2O_3-resistant APL cells. **R** The percentage of human leukemia cells in spleens of As_2O_3-resistant PDX mice with the indicated treatment was analyzed by flow cytometry. hCD45-positive cells were calculated with FlowJo software. **S** The percentage of CD11b-positive human leukemia cells from As_2O_3-resistant PDX mice with the indicated treatment was analyzed by flow cytometry. CD11b-positive cells were calculated with FlowJo software. **T** The percentage of apoptosis human leukemia cells from As_2O_3-resistant PDX mice with the indicated treatment was analyzed by flow cytometry. Apoptosis cells were calculated with FlowJo software.

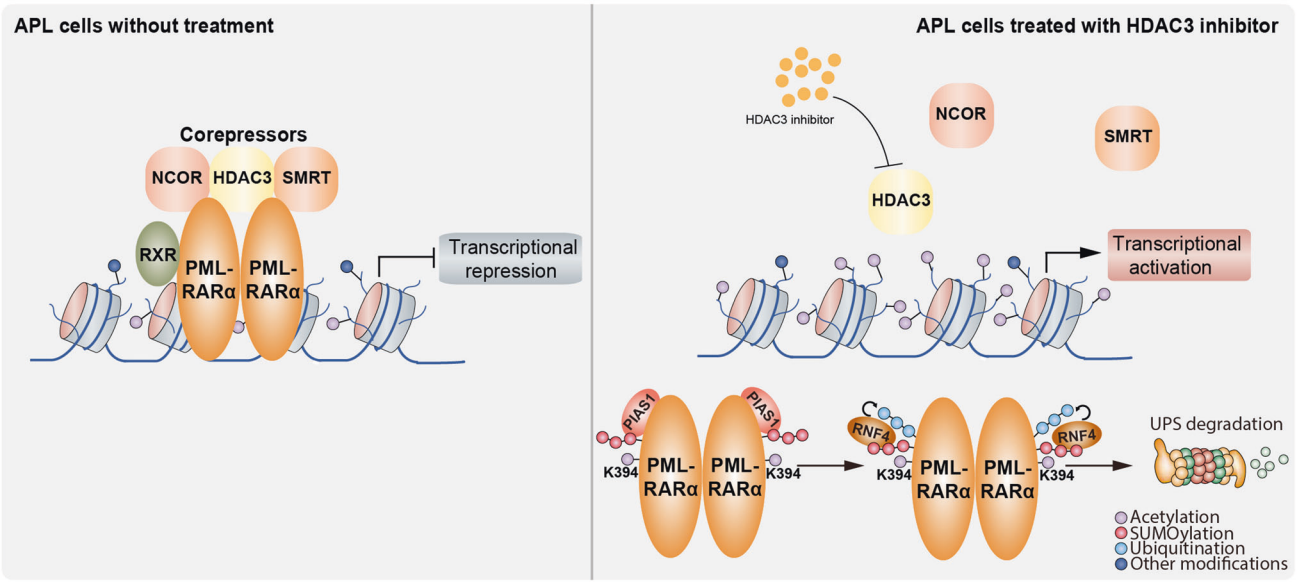

Fig. 7 Schematic diagram illustrating the mechanism by which APL is relieved through HDAC3 inhibition. PML-RARα interacts with the transcriptional inhibition complex composed of HDAC3/NCOR/SMRT to inhibit target gene transcription in APL cells. After inhibition of HDAC3, acetylation of PML-RARα lysine 394 enhances the interaction between PML-RARα and PIAS1, resulting in enhanced SUMOylation of PML-RARα and an enhanced interaction between PML-RARα and RNF4. Finally, PML-RARα is ubiquitylated by RNF4 and degraded via the ubiquitin proteasome system.

was to provide a new target for the increasing number of drug-resistant APL patients. In this study, we found that HDAC3 could maintain PML-RARα protein stability and then demonstrated that HDAC3 inhibition could relieve drug-sensitive and drug-resistant APL in vivo and in vitro. The effect of HDAC3 inhibition on APL remission was induced through degradation of wild-type PML-RARα or its mutants. Given that HDAC3 is an endogenous transcriptional repressor and a corepressor of NCOR and SMRT [16, 17], our study provides insight into APL pathogenesis: HDAC3 plays a role in maintaining PML-RARα stability.

High HDAC3 expression results in a poor prognosis in AML, suppressing transcription and differentiation in APL cells. Some studies have pointed out the important role of HDACs in APL transcription inhibition [17, 32, 33]. Our results demonstrated a greater role of HDAC3 than HDAC1 and HDAC2 in APL pathogenesis, and inhibition of HDAC3 resulted in more effective mitigation of APL. Current studies suggest that the degradation of PML-RARα depends on the SUMOylating-triggered ubiquitin proteasome pathway [25, 29]. Our work suggests that the interaction of HDAC3 and PML-RARα stabilizes the latter; inhibition of HDAC3 induces PML-RARα degradation through the ubiquitin proteasome system and relieves APL by differentiating APL cells. HDAC3 plays a role in promoting the deacetylation of substrate proteins. We found that inhibition of HDAC3 also promoted acetylation of PML-RARα, so we speculated that acetylation is the key modification to promote PML-RARα ubiquitination. It is worth

further exploring a more detailed molecular mechanism by which HDAC3 regulates PML-RARα degradation.

Treatment of APL with the ATRA/As_2O_3 combination effectively causes remission by accelerating PML-RARα degradation via the ubiquitin proteasome pathway [1, 5, 34]. However, 5–10% of APL patients relapse after CR [35] and develop resistance to ATRA and/or As_2O_3, which remains a critical clinical problem [35, 36]. Therefore, new treatment strategies should be developed for the specific clinical setting. A previous study and clinical observation revealed a series of drug-resistant PML-RARα mutations, including As_2O_3 resistance (A216V, L218P, L217F, S214L, etc.) and ATRA resistance (R276Q, R217H, G197E, S287W, etc.) [37]. Our work demonstrated that HDAC3 inhibition could relieve drug-resistant APL in vivo and in vitro by inducing APL cell differentiation and apoptosis. In addition, inhibition of HDAC3 degraded several common drug-resistant PML-RARα mutations, including A216V, L218P, R276Q, and △F286, and degraded endogenous PML-RARα mutations in ATRA-resistant cell lines. Drug-resistant APL has been a serious clinical problem to be solved, and our research provides a new target for the future treatment of relapsed/refractory APL.

In conclusion, our study proposes HDAC3 as a novel therapeutic target for the treatment of conventional and relapsed refractory APL. Targeting HDAC3 leads to the remission of APL through the differentiation and apoptosis of APL cells and the degradation of the PML-RARα fusion protein by the ubiquitin proteasome system (Fig. 7).

DATA AVAILABILITY

The dataset analyzed during this study can be accessed using the GEO with accession GSE13204. All the other data supporting the findings of this study are available within the article and its supplementary information files and from the corresponding author upon reasonable request.

REFERENCES

1. de The H, Pandolfi PP, Chen Z. Acute promyelocytic leukemia: a paradigm for oncoprotein-targeted cure. Cancer Cell. 2017;32:552–60.
2. Zhu J, Zhou J, Peres L, Riaucoux F, Honore N, Kogan S, et al. A sumoylation site in PML/RARA is essential for leukemic transformation. Cancer Cell. 2005;7:143–53.
3. Chen ZH, Wang WT, Huang W, Fang K, Sun YM, Liu SR, et al. The lncRNA HOTAIRM1 regulates the degradation of PML-RARA oncoprotein and myeloid cell differentiation by enhancing the autophagy pathway. Cell Death Differ. 2017;24:212–24.
4. Xu HE, Stanley TB, Montana VG, Lambert MH, Shearer BG, Cobb JE, et al. Structural basis for antagonist-mediated recruitment of nuclear co-repressors by PPARα. Nature. 2002;415:813–7.
5. Lo-Coco F, Avvisati G, Vignetti M, Thiede C, Orlando SM, Iacobelli S, et al. Retinoic acid and arsenic trioxide for acute promyelocytic leukemia. N. Engl J Med. 2013;369:111–21.
6. Zhang XW, Yan XJ, Zhou ZR, Yang FF, Wu ZY, Sun HB, et al. Arsenic trioxide controls the fate of the PML-RARalpha oncoprotein by directly binding PML. Science (N. Y, NY). 2010;328:240–3.
7. Shen ZX, Shi ZZ, Fang J, Gu BW, Li JM, Zhu YM, et al. All-trans retinoic acid/As2O3 combination yields a high quality remission and survival in newly diagnosed acute promyelocytic leukemia. Proc Natl Acad Sci USA. 2004;101:5328–35.
8. Nowak D, Stewart D, Koeffler HP. Differentiation therapy of leukemia: 3 decades of development. Blood. 2009;113:3655–65.
9. Rochette-Egly C, Germain P. Dynamic and combinatorial control of gene expression by nuclear retinoic acid receptors (RARs). Nucl Recept Signal. 2009;7:e005.
10. Platzbecker U, Avvisati G, Cicconi L, Thiede C, Paoloni F, Vignetti M, et al. Improved outcomes with retinoic acid and arsenic trioxide compared with retinoic acid and chemotherapy in non-high-risk acute promyelocytic leukemia: final results of the randomized Italian-German APL0406 trial. J Clin Oncol: Off J Am Soc Clin Oncol. 2017;35:605–12.
11. Kayser S, Schlenk RF, Platzbecker U. Management of patients with acute promyelocytic leukemia. Leukemia. 2018;32:1277–94.
12. Johnstone RW. Histone-deacetylase inhibitors: novel drugs for the treatment of cancer. Nat Rev Drug Discov. 2002;1:287–99.
13. Yang XJ, Seto E. The Rpd3/Hda1 family of lysine deacetylases: from bacteria and yeast to mice and men. Nat Rev Mol Cell Biol. 2008;9:206–18.
14. Zhu J, Chen Z, Lallemand-Breitenbach V, de Thé H. How acute promyelocytic leukaemia revived arsenic. Nat Rev Cancer. 2002;2:705–13.
15. Zhou J, Pérès L, Honoré N, Nasr R, Zhu J, de Thé H. Dimerization-induced corepressor binding and relaxed DNA-binding specificity are critical for PML/RARA-induced immortalization. Proc Natl Acad Sci USA. 2006;103:9238–43.
16. Karagianni P, Wong J. HDAC3: taking the SMRT-N-CoRrect road to repression. Oncogene. 2007;26:5439–49.
17. Zhang J, Kalkum M, Chait BT, Roeder RG. The N-CoR-HDAC3 nuclear receptor corepressor complex inhibits the JNK pathway through the integral subunit GPS2. Mol Cell. 2002;9:611–23.
18. Mehdipour P, Santoro F, Botrugno OA, Romanenghi M, Pagliuca C, Matthews GM, et al. HDAC3 activity is required for initiation of leukemogenesis in acute promyelocytic leukemia. Leukemia. 2017;31:995–7.
19. Moretti S, Abdel-Aziz AK, Ceccacci E, Pallavicini I, Santoro F, de Thé H, et al. Co-targeting leukemia-initiating cells and leukemia bulk leads to disease eradication. Leukemia. 2022;36:1306–12.
20. Long J, Jia MY, Fang WY, Chen XJ, Mu LL, Wang ZY, et al. FLT3 inhibition upregulates HDAC8 via FOXO to inactivate p53 and promote maintenance of FLT3-ITD + acute myeloid leukemia. Blood. 2020;135:1472–83.
21. Rabellino A, Carter B, Konstantinidou G, Wu SY, Rimessi A, Byers LA, et al. The SUMO E3-ligase PIAS1 regulates the tumor suppressor PML and its oncogenic counterpart PML-RARA. Cancer Res. 2012;72:2275–84.
22. Shao X, Chen Y, Wang W, Du W, Zhang X, Cai M, et al. Blockade of deubiquitinase YOD1 degrades oncogenic PML/RARα and eradicates acute promyelocytic leukemia cells. Acta Pharm Sin B. 2022;12:1856–70.
23. Hu C, Peng K, Wu Q, Wang Y, Fan X, Zhang DM, et al. HDAC1 and 2 regulate endothelial VCAM-1 expression and atherogenesis by suppressing methylation of the GATA6 promoter. Theranostics. 2021;11:5605–19.
24. Long J, Fang WY, Chang L, Gao WH, Shen Y, Jia MY, et al. Targeting HDAC3, a new partner protein of AKT in the reversal of chemoresistance in acute myeloid leukemia via DNA damage response. Leukemia. 2017;31:2761–70.
25. Li K, Wang F, Cao WB, Lv XX, Hua F, Cui B, et al. TRIB3 promotes APL progression through stabilization of the oncoprotein PML-RARalpha and inhibition of p53-mediated senescence. Cancer cell. 2017;31:697–710.e697.
26. Hu J, Zhang H, Li J, Jiang X, Zhang Y, Wu Q, et al. ROCK1 activation-mediated mitochondrial translocation of Drp1 and cofilin are required for arnidiol-induced mitochondrial fission and apoptosis. J Exp Clin Cancer Res. 2020;39:37.
27. Deng X, Liu J, Liu L, Sun X, Huang J, Dong J. Drp1-mediated mitochondrial fission contributes to baicalein-induced apoptosis and autophagy in lung cancer via activation of AMPK signaling pathway. Int J Biol Sci. 2020;16:1403–16.
28. Nguyen HCB, Adlanmerini M, Hauck AK, Lazar MA. Dichotomous engagement of HDAC3 activity governs inflammatory responses. Nature. 2020;584:286–90.
29. Lallemand-Breitenbach V, Jeanne M, Benhenda S, Nasr R, Lei M, Peres L, et al. Arsenic degrades PML or PML-RARalpha through a SUMO-triggered RNF4/ubiquitin-mediated pathway. Nat Cell Biol. 2008;10:547–55.
30. Goto E, Tomita A, Hayakawa F, Atsumi A, Kiyoi H, Naoe T. Missense mutations in PML-RARA are critical for the lack of responsiveness to arsenic trioxide treatment. Blood. 2011;118:1600–9.
31. de The H, Le Bras M, Lallemand-Breitenbach V. The cell biology of disease: Acute promyelocytic leukemia, arsenic, and PML bodies. J Cell Biol. 2012;198:11–21.
32. Minucci S, Nervi C, Lo Coco F, Pelicci PG. Histone deacetylases: a common molecular target for differentiation treatment of acute myeloid leukemias? Oncogene. 2001;20:3110–5.
33. Matthews GM, Mehdipour P, Cluse LA, Falkenberg KJ, Wang E, Roth M, et al. Functional-genetic dissection of HDAC dependencies in mouse lymphoid and myeloid malignancies. Blood. 2015;126:2392–403.
34. Zhu J, Gianni M, Kopf E, Honoré N, Chelbi-Alix M, Koken M, et al. Retinoic acid induces proteasome-dependent degradation of retinoic acid receptor alpha (RARalpha) and oncogenic RARalpha fusion proteins. Proc Natl Acad Sci USA. 1999;96:14807–12.
35. Wang X, Lin Q, Lv F, Liu N, Xu Y, Liu M, et al. LG-362B targets PML-RARalpha and blocks ATRA resistance of acute promyelocytic leukemia. Leukemia. 2016;30:1465–74.
36. Lu Y, Yan JS, Xia L, Qin K, Yin QQ, Xu HT, et al. 2-Bromopalmitate targets retinoic acid receptor alpha and overcomes all-trans retinoic acid resistance of acute promyelocytic leukemia. Haematologica. 2019;104:102–12.
37. Zhu HH, Qin YZ, Huang XJ. Resistance to arsenic therapy in acute promyelocytic leukemia. N Engl J Med. 2014;370:1864–6.

AUTHOR CONTRIBUTIONS

JH, KL, BD, and FW designed the overall study and wrote the manuscript; BD and YW performed experiments and analyzed data; JZ, YL, and TZ helped with animal experiments; LZ, LW and WG helped to collect patients' primary samples; JL and HZ provided advice and reviewed the manuscript.

FUNDING

This work was supported by grants from the National Key R&D Program of China (2022YFA1106100), the National Natural Science Foundation of China (81770187,

82170149, 82222070, 82273973, 81872904, 82073887, 82073711 and 82003798), the CAMS Innovation Fund for Medical Sciences (2021-I2M-1-030, 2022-I2M-2-002 to KL; 2021-I2M-1-070 to TTZ) and the Fundamental Research Funds for the Central Universities (2022-RC350-07, 3332022149).

COMPETING INTERESTS

The authors declare no competing interests.

ETHICS APPROVAL

The study was approved by the Institutional Review Board of the Ruijin Hospital, Shanghai Jiao Tong University School of Medicine. All animal procedures were approved by the Institutional Committee for the Ethics of Animal Care and Treatment in Biomedical Research of Chinese Academy of Medical Sciences and PUMC.

ADDITIONAL INFORMATION

Supplementary information The online version contains supplementary material available at https://doi.org/10.1038/s41418-023-01139-8.

Correspondence and requests for materials should be addressed to Ke Li or Jiong Hu.